

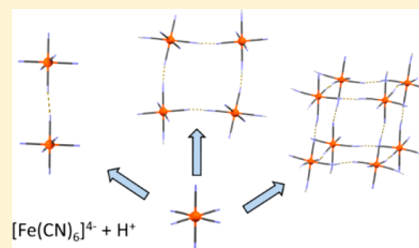
New Tricks by Old Anions: Hydrogen Bonded Hexacyanoferrous Anionic Networks

Ivica Cvrtila[†] and Vladimir Stilinović*[‡]

Department of Chemistry, Faculty of Science, University of Zagreb, Horvatovac 102a, HR-10002 Zagreb, Croatia

Supporting Information

ABSTRACT: Hexacyanoferrates are well-known to form metal–organic frameworks by coordination to metal atoms or acting as hydrogen bond acceptors. In this paper we report a new type of hexacyanoferrate self-assembly, based on direct hydrogen bonding of partially protonated hexacyanoferrate anions. By preparing a series of 15 hexacyanoferrates with various organic bases, we have found that protonated hexacyanoferrates (present in 10 structures) readily form chains (two structures), two-dimensional (four structures), or three-dimensional networks (four structures), whereby the dimensionality of the network generally increases with the protonation degree of the hexacyanoferrates. The exact mode of the self-assembly, including the network type, depends on fine interplay of the pK_a value of the base, its steric properties, and the stoichiometry of the formed solid.

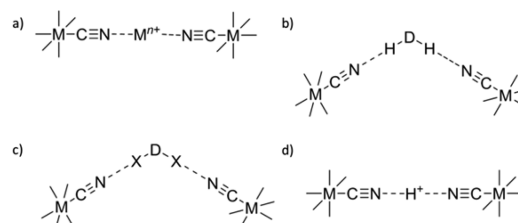


INTRODUCTION

Hexacyanoferrates (HCFs) have a special place in chemistry ever since the accidental discovery of Prussian blue ca. 1703, and preparation of potassium hexacyanoferrate(II) (*gelbes Blutlaugensalz*) in 1752.^{1–3} After centuries of the use of Prussian blue as a pigment, and decades of intense study of its structure, physical and chemical properties,^{4–9} recent advances in crystal engineering and materials chemistry have led to an explosion of the diversity of Prussian blue analogues, as such compounds can act as electrode materials,^{10–16} molecular magnets,^{17–24} or photoswitchable magnetic solids,^{25–29} and can also be applied as molecular sieves,^{30–32} antidotes or decontaminants for radioactive metals,^{33–35} and for gas storage.^{36–39} Design of these compounds generally relies on formation of coordination networks of polycyanometalate (PCM) anions and metal cations, as well as on hydrogen bonding between the PCMs and organic proton donors. The transition from purely inorganic to metal–organic frameworks (MOFs) broadens the scope of properties of these materials and allows for their fine-tuning, which are necessary requirements for the rational design of functional materials.

The design of PCM based structures is primarily based on the ability of such anions to act as (multiple) electron pair donors. This property enables them to act as (bridging) ligands for metal cations (Scheme 1a), which can lead to discrete clusters or polymeric structures.^{21,40–56} However, the electron-donating potential of PCMs is not limited to formation of coordinative bonds. Several material design strategies have been devised based on hydrogen bonding of PCM (most commonly HCF) anions with organic hydrogen donors (Scheme 1b). In such structures, the finite or infinite structures are formed by interposing organic functions or molecules, rather than metal cations, between PCM anions.^{54,57–66} Bridging PCM units by multiple proton donors may lead to formation of specific

Scheme 1. Basic Types of Connecting PCMs: (a) Metal Coordination; (b) Bridging by Hydrogen Bond Donors; (c) Bridging by Halogen Bond Donors; (d) Bridging by Protons (This Work)



structural motifs, such as chains or 2D networks, which can be used to control their self-assembly, as best shown by preparation of isostructural compounds.⁶⁰ A more recent, although essentially equivalent, strategy employed in the design of PCM based MOFs is based on the potential of metal-bound cyanide to act as a halogen acceptor and form halogen bonds with iodo- and bromo-derivatized organic cations (Scheme 1c).^{67–70}

The versatility of PCMs as electron donors (Lewis bases) in materials design leads to an interesting question—is it possible to devise a design strategy which would employ them in some fundamentally different manner? A possible method would be to use partially protonated PCMs which could simultaneously act as electron and proton donors (Scheme 1d). A strong indication of the viability of such a strategy is the presence of extremely strong hydrogen bonds formed by metal bound HNC ligands, particularly in the case of ionic $[M-CN\cdots H\cdots$

Received: September 25, 2017

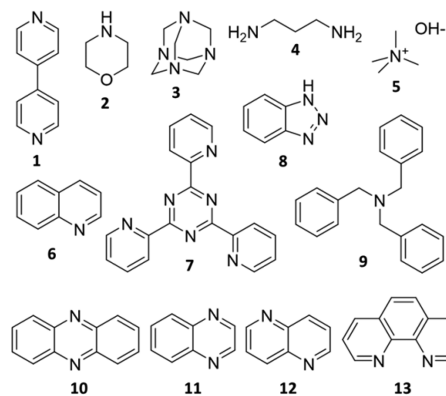
Revised: November 7, 2017

Published: November 13, 2017

NC—M][−] complexes.^{71,72} Therefore, despite the current scarcity of such compounds in the literature,^{73–82} it is possible that an entire new family of materials may be designed on the basis of hydrogen bonded poly(hydrogenpolycyanometalate) anionic architectures.

Protonation of PCM anions can in principle be achieved in two manners: by acidifying a solution of an alkali metal PCM salt, or by using a PCM acid as the source of the (protonated) anions. We have opted for the latter method, which, in spite of involving an additional step in the synthesis (preparation and isolation of the acid), has significant advantages: PCM acids are usually more soluble in organic solvents than the corresponding salts, which widens the range of organic bases that can be used. Also the introduction of additional ions into the system is avoided, thus enabling better control over the composition of the final product. For this study we have employed stable and easily synthesized hexacyanoferric(II) acid (H₄[Fe(CN)₆]).⁸³ The acid was crystallized with a variety of organic bases spreading over a wide range of basicities and steric properties (Scheme 2). Although H₄[Fe(CN)₆] is very strong in the first

Scheme 2. Organic Bases Used in This Research: 4,4′-Bipyridine (1), Morpholine (2), Urotropine (3), 1,3-Diaminopropane (4), Tetramethylammonium Hydroxide (5), Quinoline (6), 2,4,6-Tris(pyrid-2-yl)-1,3,5-triazine (7), Benzotriazole (8), Tribenzylamine (9), Phenazine (10), Quinoxaline (11), 1,5-Naphthyridine (12), and Phenanthroline (13)



two dissociation stages (pK_{a1} and pK_{a2} are too low to be determined), and can hardly be expected to exist in the fully protonated form even when crystallized with very weak organic bases, relatively low values of subsequent dissociation constants ($pK_{a3} = 2.2 \pm 0.2$; $pK_{a4} = 4.17 \pm 0.02$)⁸⁴ render the presence of H₂[Fe(CN)₆]^{2−} and H[Fe(CN)₆]^{3−} anions likely in the crystal structures of organic HCFs.

RESULTS AND DISCUSSION

By crystallizing H₄[Fe(CN)₆] with 13 organic bases we have obtained 15 distinct solids (Table 1). In 10 of them protonated HCF species were found. The most commonly appearing was the expected H₂[Fe(CN)₆]^{2−} ion found in six structures, while the other expected species, H[Fe(CN)₆]^{3−}, was found only in one structure. Surprisingly, as many as four structures comprise the highly acidic H₃[Fe(CN)₆][−]. Hydrogen bonding pattern changes with the protonation state: in XII and XV only HCF–HCF hydrogen bonds are present, in VI–XI, XIII, and XIV they are partly replaced by hydrogen bonds to other species, while the fully deprotonated [Fe(CN)₆]^{4−} anions in I–V, being

exclusively hydrogen bond acceptors, formed hydrogen bonds only with other species.

Presence of protonated HCFs invariably leads to formation of hydrogen bonded polyanionic architectures, and the dimensionality of the architecture is determined primarily by the protonation state – H[Fe(CN)₆]^{3−} anions can only assemble into chains, while H₂[Fe(CN)₆]^{2−} and H₃[Fe(CN)₆][−] anions, depending on the spatial arrangement of the protons, may form 2D sheets or 3D networks. Thus, in I–V, where the anions can only act as hydrogen bond acceptors, complex hydrogen bonded networks are present (network type ‘a’ in Table 1, an example shown in Figure 1), comprising [Fe(CN)₆]^{4−} anions bridged by multiple hydrogen bond donors (Figures 1a, 2c,d, and 4). H[Fe(CN)₆]^{3−} anions in VI, as well as alternating [Fe(CN)₆]^{4−} and H₂[Fe(CN)₆]^{2−} anions in VII, form {H[Fe(CN)₆]^{3−}}_n chains (type ‘b’), which are further connected by water molecules (Figures 1b, 3c,d, and 5c). H₂[Fe(CN)₆]^{2−} anions in VIII, IX, and XI, as well as H₃[Fe(CN)₆][−] anions in X, form 2D sheets (type ‘c’), which form separate layers, with cations and other molecules attached as pendants (Figures 1c, 2b, and 3a,b). The same anions, H₂[Fe(CN)₆]^{2−} in XIII, and H₂[Fe(CN)₆]^{2−} and H₃[Fe(CN)₆][−] in XIV, in different relative orientations, form truncated 3D cuboid networks (type ‘d’), again with the cations attached as pendants (Figures 1d and 5a). Finally, H₃[Fe(CN)₆][−] anions in XII and XV form 3D cuboid networks (type ‘e’) comprising exclusively HCF–HCF hydrogen bonds, while the cations and solvent molecules are hosted within the cavities of the networks (Figures 1e and 6b,d).

The natural path toward the control of the network type therefore appears to be using organic bases of different basicities in order to control the protonation state of the HCF anions (see Figures S71 and S72). Indeed, H₃[Fe(CN)₆][−] anions are primarily found in the cases when very weak organic bases were used (10 and 11), while stronger bases (2, NH₃, 4, and 5) lead to structures with the fully deprotonated [Fe(CN)₆]^{4−} anions (Table 1). However, the effect of the base pK_a is far from straightforward—there does not seem to be any statistically significant difference between the base pK_a span where H₃[Fe(CN)₆][−] (0.56–4.98), H₂[Fe(CN)₆]^{2−} (0.56–5.32), or H[Fe(CN)₆]^{3−} anions (2.27–4.94) are present in the structures, and while it would seem that protonated HCF anions will rarely be found when bases with $pK_a > 5$ are used (with the exception of the sterically demanding 9), 1 with $pK_a < 5$ leads to fully deprotonated [Fe(CN)₆]^{4−} anions. It is therefore evident that other factors also have a significant influence on the protonation state of the HCF anions, as well as the resulting hydrogen bonding architectures.

Among these, most noticeable are the effects of the hydrogen bonding and steric effects. Thus, in VIII and I the cations bridge the anions via multiple hydrogen bonds, but with different distances between the hydrogen atoms involved in hydrogen bonds (hydrogen atom spans), which affects both the protonation state and the dimensionality of the HCF network. The hydrogen atom span of the H8⁺ cations in VIII (ca. 3.6 Å) fits the period of the 2D {H₂[Fe(CN)₆]^{2−}}_n network (Figure 2a), so that they easily hydrogen bond to neighboring H₂[Fe(CN)₆]^{2−} anions, thus forming zigzag chains over and below the HCF layers (Figure 2b). As a consequence, the 2D network is stabilized. This stabilization through bridging by the cation may also account for the lower protonation state of the acid in VIII as compared to X and XII, even though 8 and 10 are bases of similar strength (Table 1). The longer H₂I²⁺

Table 1. Overview of the Prepared Compounds

compound	base, pK _a (B)	B: HCF ^a	product composition	network ^b
I	1, 4.85/4.92 ⁸⁵	2:1	(H ₂ I) ₂ HCF(H ₂ O) ₄	a (0D)
II	2, 8.36 ⁸⁶	4:1	(H ₂) ₄ HCF(H ₂ O) ₄	a (0D)
III	3/NH ₃ , 4.89/9.25 ⁸⁷	4:1	(H ₃) ₂ (NH ₄) ₂ HCF(H ₂ O) ₄ ^c	a (0D)
IV	4, 8.55/10.65 ⁸⁸	4:1	(4-CO ₂) ₂ (H ₂) ₂ HCF(H ₂ O) ₂ ^d	a (0D)
V ^e	5, 7 (H ₂ O)	4:1	(Me ₄ N) ₂ (H ₃ O) ₂ HCF	a (0D)
VI	6, 4.94 ⁸⁹	4:1 (MeOH)	(H ₆) ₃ (HHCF)(H ₂ O) ₂	b (1D)
VII	7, 2.72/3.55 ⁹⁰	1:1 (MeOH)	(H ₂) ₇ (H ₃ O) ₂ (H ₂ HCF)HCF(H ₂ O) ₁₃	b (1D)
VIII	8, 1.6 ⁸⁹	2:1 (MeOH)	(H ₈) ₂ (H ₂ HCF)	c (2D)
IX	9, 5.32 ⁹¹	2:1 (MeOH)	(H ₉) ₂ (H ₂ HCF)(MeOH) ₂	c (2D)
X	10, 1.23 ⁸⁹	5:1 (EtOH)	(H ₃ O) ₂ (H ₃ HCF) ₂ 10 ₃ (H ₂ O) ₆	c (2D)
XI	11, 0.56 ⁹²	4:1 (MeOH)	(H ₁₁) ₄ (H ₂ HCF) ₂ 11	c (2D)
XII	10, 1.23	1:1 (MeOH)	(H ₁₀) ₂ (H ₃ HCF) ₂ 10(MeOH) ₂	e (3D)
XIII	12, 2.91 ⁹²	2:1	(H ₁₂) ₂ (H ₂ HCF)	d (3D)
XIV	13, 4.98 ⁹³	2:1 (MeOH)	(H ₁₃) ₂ (H ₂ HCF)(H ₃ HCF)13	d (3D)
XV	11, 0.56	4:1 (MeOH)	(H ₁₁)(H ₃ HCF)11(H ₂ O) ₂	e (3D)

^aStoichiometric ratio of the reactants used for the synthesis. Water is always used as a solvent; cosolvent, if any, is noted in parentheses. ^bNetwork types refer to Figure 1, where examples are presented; 0D means discrete HCF anions. ^cNH₄⁺ cations formed by decomposition of 3 in acidic solution. ^d4-CO₂ carbamate zwitterions formed from 4 and atmospheric CO₂. ^eHCF(III), likely formed due to oxidation by atmospheric oxygen.

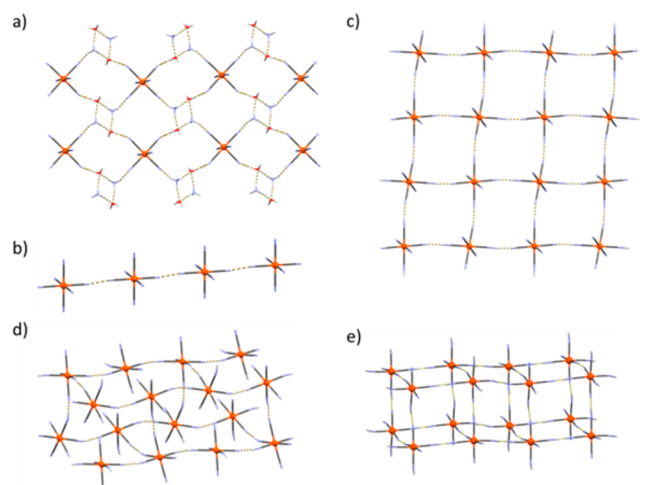


Figure 1. Examples of types of HCF architectures: (a) type 'a': HCF acting as hydrogen bond acceptor only ([Fe(CN)₆]⁴⁻ anions bridged by hydrogen bond donors in the structure of III); (b) type 'b': 1D chain of H[Fe(CN)₆]³⁻ anions (in VI); (c) type 'c': 2D network of H₂[Fe(CN)₆]²⁻ anions (in IX); (d) type 'd': truncated 3D network of H₂[Fe(CN)₆]²⁻ anions (in XIII); (e) type 'e': cuboid 3D network of H₃[Fe(CN)₆]⁻ anions (in XII).

cations in I (hydrogen atom span ca. 8.7 Å) push the anions from one another and water molecules are interpolated in between (Figure 2c). This leads to full deprotonation of the acid despite the intermediate basicity of I and to formation of a HCF-water network (Figure 2d), instead of (exclusively) a HCF network, such as present in VIII (and also in IX–XI).

Unlike in the previous examples where HCF architecture was determined by hydrogen bonding abilities of the base molecules, in VII and IX the effect of basicity upon the protonation state and self-assembly of the HCF anions is overcome by the size of the cations. The large H₉⁺ cations in IX (Figure 3a) are compelled to form separate layers (Figure 3b), which in turn facilitates formation of the 2D network of H₂[Fe(CN)₆]²⁻ anions (in contrast to I, where hydrogen bonding led to interpolation of water between the HCF anions and full deprotonation). The H⁷⁺ cations in VII are also too

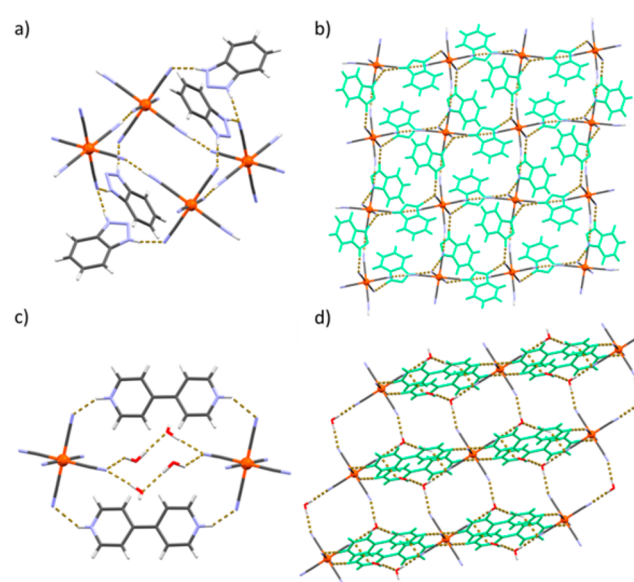


Figure 2. Effects of hydrogen bonding upon the architecture of HCFs: (a) H₈⁺ cations bridging H₂[Fe(CN)₆]²⁻ anions, resulting in type 'c' connectivity (VIII); (b) 2D HCF network with the H₈⁺ cations (green) attached (VIII); (c) interpolation of water between [Fe(CN)₆]⁴⁻ anions bridged by H₂I²⁺ cations, resulting in type 'a' connectivity (I); (d) H₂I⁺ cations (green) bridging the HCF anions in the HCF–water network (I).

large to fit into cavities of 3D or 2D networks, while the position of the proton on 2-pyridyl group (see Scheme 2) hinders the approach of the anion and thus prevents formation of HCF layers hydrogen bonded to the cations. Thus, only H[Fe(CN)₆]³⁻ chains are allowed to form (with water molecules interpolated between the chains; Figure 3c), while at the same time a significant amount of the cell space is filled by polymeric water clusters (Figure 3d).

Possibly the most pronounced example of the hydrogen bonding and steric effects is V, derived from 5 and HCF(III). As 5 is a hydroxide, the strongest base possible in aqueous environments, full deprotonation of the acid is expected. However, although the anions indeed are fully deprotonated

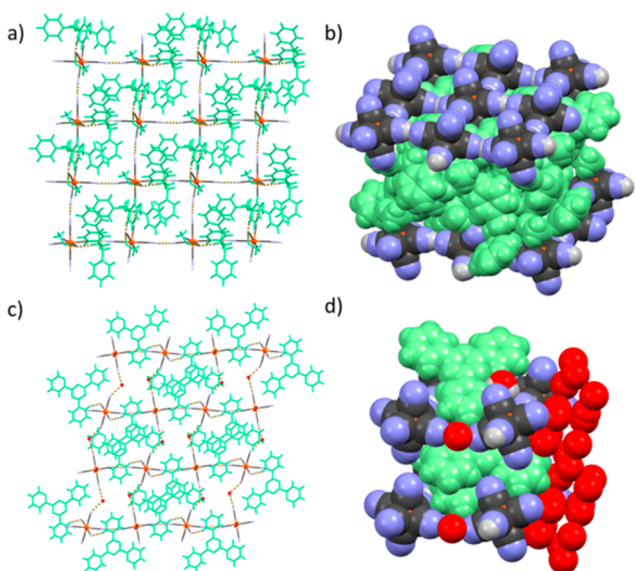


Figure 3. Steric effects upon the architecture of HCFs: (a) bulky H9^+ cations (green) hydrogen bonded to the 2D HCF network (IX; 'c' type connectivity); (b) double layer of H9^+ cations (green) between the HCF networks (IX); (c) H7^+ cations attached to the HCF chains bridged by water molecules (VII; 'b' type connectivity); (d) H7^+ cations stacked between the HCF chains connected by polymeric water clusters (VII; water molecules represented by oxygen atoms only).

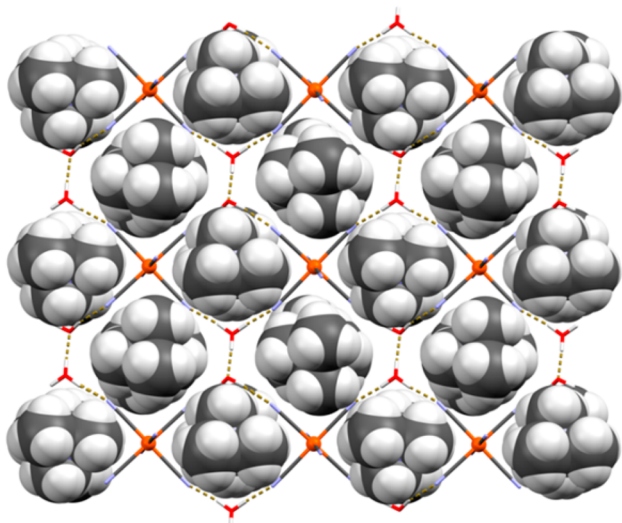


Figure 4. HCF-Zundel 2D network (type 'a' connectivity) hosting bulky Me_4N^+ cations (V).

and consequently not directly hydrogen bonded, they are bridged by $(\text{H}_5\text{O}_2)^+$ (Zundel) cations, altogether forming a 2D network equivalent to those in VIII–XI, but with one-half HCF anions replaced by $(\text{H}_5\text{O}_2)^+$ cations (Figure 4, compare with Figure 1c). The presence of $(\text{H}_5\text{O}_2)^+$ cations (one of the “hydrates” of H^+ present in aqueous acids) in a compound crystallized from a hydroxide solution, strongly contrasts the supposition that the deprotonation of HCF anion occurred because of the presence of a strong base (OH^- ; note that reaction conditions – Table 1 – were such that there was sufficient amount of base to completely neutralize the acid). Instead, the structure appears to be essentially a 2D network of $[\text{H}[\text{Fe}(\text{CN})_6]^{2-}]$ anions with two water molecules per anion

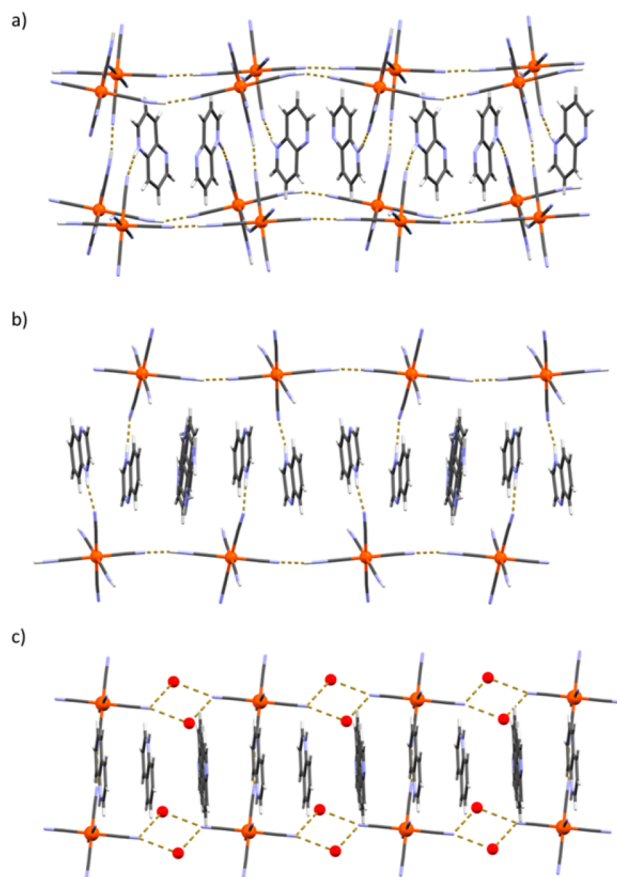


Figure 5. Effects of base content upon the HCF architecture in a series of structures derived from bicyclic aromatic bases: (a) two protonated molecules of 12 per HCF unit neatly fit the network in XIII, with anions forming a 3D hydrogen bonded network of type 'd' connectivity; (b) in XI, the base/HCF ratio is increased to 5/2 by interpolation of disordered neutral molecules of 11, disrupting the hydrogen bonding in one direction (the structure comprises hydrogen bonded HCF layers (type 'c' connectivity), parallel to the direction of viewing); (c) further increase of the base to HCF ratio to 3 by doubling the number of interpolated neutral base (6) molecules in VI disrupts a second series of hydrogen bonds, causing interpolation of water molecules between the HCF ions, leaving only hydrogen bonded HCF chains (along the direction of viewing), belonging to the type 'b' connectivity.

interpolated into the hydrogen bonding system. Such enlargement of the $\{\text{H}[\text{Fe}(\text{CN})_6 \cdot 2\text{H}_2\text{O}]_n^{2n-}\}$ hydrogen bonded network is necessary in order to enlarge the space between the terminal cyano groups sufficiently to accommodate the bulky Me_4N^+ cations.

Base content, i.e., base to HCF ratio, can also influence the protonation state through steric effects upon the self-assembly of the HCF anions. This is best demonstrated by the salts of planar aromatic bases (6, 10, 11, 12, and 13), particularly within a series of salts of sterically identical bicyclic bases (6, 11, and 12; Figure 5). The structures of salts with lower base content—3/2 (XII and XIV) or 2 (XIII and XV) base molecules per HCF anion—comprise 3D hydrogen bonded HCF networks, with base molecules neatly filling the voids (Figures 5a and 6b,d). Increasing the base to HCF ratio to 5/2 (X and XI) disrupts hydrogen bonding of anions in one direction, resulting in 2D layers hydrogen bonded to protonated base molecules (Figure 5b). This happens

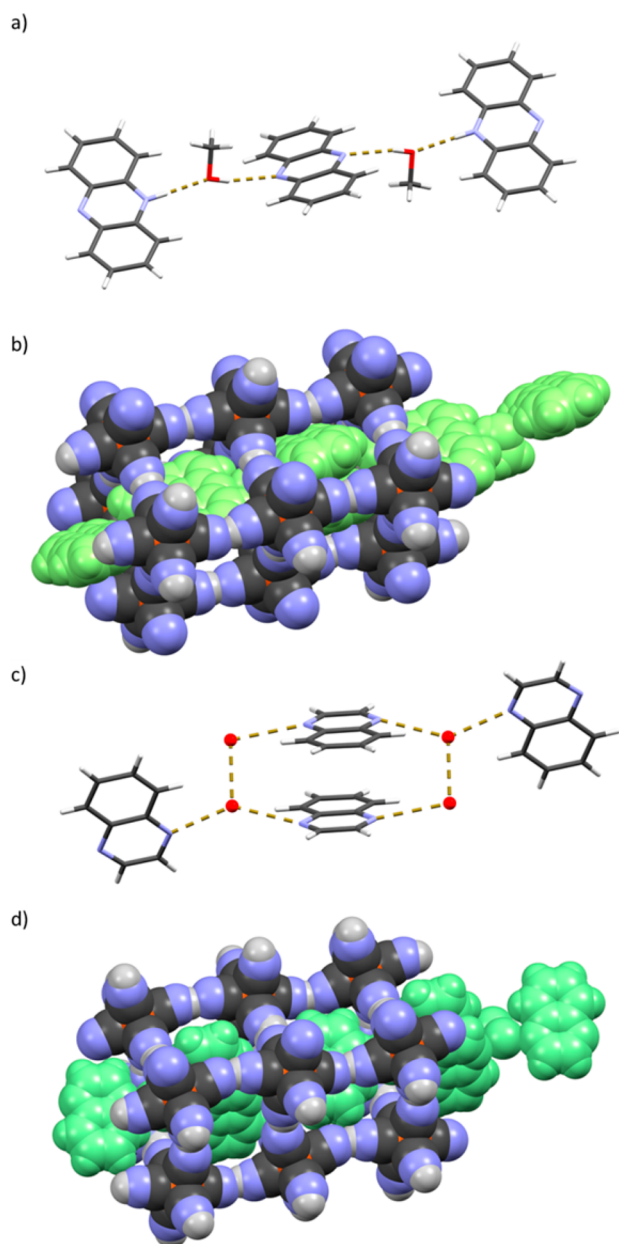


Figure 6. Supramolecular oligomers formed by hydrogen bonding between (protonated) base and solvent molecules: (a) (MeOH)₂(10)-(H10⁺)₂ pentamer in XII; (b) the pentamers as guests to the 3D HCF network (type ‘e’ connectivity); (c) (H₂O)₄(11)₂(H11⁺)₂ octamer in XV (water molecules represented as oxygen atoms only); (d) the octamers as guests to the 3D HCF network (type ‘e’ connectivity).

regardless of the protonation state of the HCF anions, as XI comprises H₂[Fe(CN)₆]²⁻ anions, while X comprises H₃[Fe(CN)₆]⁻ anions. Although the latter are able to build the cuboid 3D assembly, the stacked base molecules separate the HCF layers in both structures. A further increase of the ratio to 3:1 in VI disrupts a second series of hydrogen bonds and leads to interpolation of water molecules (cf. structure of I described above), leaving only 1D hydrogen bonded chains of H[Fe(CN)₆]³⁻ anions (Figure 5c). It is also noteworthy that the increase of base content may affect the hydrogen bonding of the HCF anions, without necessarily changing their protonation state—e.g., both XI and XIII comprise H₂[Fe(CN)₆]²⁻ anions, although their base content, as well as hydrogen bonded HCF

network differ—as additional base molecules may be interpolated as neutral molecules. The presence of neutral base molecules is indeed a common feature in all structures found to have hydrogen bonded HCF networks as they appear in 6 (VI, X, XI, XII, XIV, and XV) out of 10 (VI–XV) structures with direct hydrogen bonds between HCF anions. On the other hand, none of the structures comprising isolated HCF anions were found to contain neutral base molecules.

Taken together, these examples imply that the existence of a given protonated HCF species in a crystal structure is not simply a matter of the base strength. The supramolecular surroundings of the anion, i.e., the base size and shape, as well as its relative amount, also must be taken into account when designing a HCF material as they sometimes may even overcome the effect of the base strength. Practical implementation of these criteria is best exemplified by the comparing the structures comprising 3D HCF networks (XII–XV).

The cuboid 3D network of hydrogen bonded HCF anions observed in XII and XV, with undisturbed chains of nearly linear hydrogen bonds in all three directions, can be considered the ideal state of the HCF network, as the cyano groups are exclusively hydrogen bonded with each other so that each HCF anion forms six symmetric hydrogen bonds with six neighbors. For such a structure to form, H₃[Fe(CN)₆]⁻ anions must be present in sufficient quantities, while the cations, and possibly other molecules, must fit the voids of the network, effectively acting as guests. Using weak aromatic bases, such as 10 or 11, meets both criteria. They are sufficiently weak bases to obtain the necessary H₃[Fe(CN)₆]⁻ anions. At the same time, neutral base molecules may act as hydrogen bond acceptors and participate in forming supramolecular complexes of cations, base, and solvent molecules, such as (MeOH)₂(10)(H10⁺)₂ clusters in XII (Figure 6a) and (H₂O)₄(11)₂(H11⁺)₂ in XV (Figure 6c). These supramolecular clusters comprise alternating bulged (base molecules) and thin (solvent molecules) regions which allow them to spread through several (in both cases three) “cells” of the [H₃[Fe(CN)₆]⁻]_n network and are also sufficiently flexible to accommodate to the interior of the network in order to neatly fit the voids (Figure 6b,d). It is interesting to note that in both cases the structures comprise both strongly acidic H₃[Fe(CN)₆]⁻ anions and neutral base molecules, demonstrating the dominant effect of hydrogen bonding (both within the network and within the cation–solvent–base clusters) over the acid–base speciation expected on the basis of pK_a values. However, this dominance is lost when stronger bases are used—12 in XIII and 13 in XIV (Figure 5a). This still allows for formation of 3D networks, but here the network is truncated due to further deprotonation of the HCF anions and hydrogen bonding to the cations, which in turn do not form clusters with additional neutral base or solvent molecules.

Importance of the appropriate guest for stabilization of 3D networks is also well illustrated by the crystal structures of HCF acids themselves. In all the known structures thereof there are 3D HCF networks present, but often heavily distorted. In anhydrous hexacyanoferric(II) acid⁷⁵ there are four protons per acid molecule so the cuboid 3D network, which requires exactly three, cannot form. This still allows for formation of a 2D network similar to those in VIII–XI, while the connectivity along the third dimension is achieved by uncommon hydrogen bonds with the donating hydrogen cyanide groups being perpendicular to the accepting ones. In the hydrates of hexacyanoferric(III) acid,^{76–80} there are three protons per

HCF moiety so that the 3D structure should be easily formed. However, the 3D networks are in all cases distorted or even truncated, as water acts as a base and forms various protonated clusters. Conversely, in anhydrous hexacyanoferric(III) acid,^{76,77} as well as in related hexacyanocobaltic(III) acid,^{81,82} there are cuboid 3D networks present, though not stabilized by guests, but by 3-fold interpenetration of the cuboid networks.

CONCLUSIONS

The structures of the prepared series of organic hexacyanoferrates show that the potential of the HCFs to assemble into 2D or 3D networks is not limited to metal coordination and hydrogen or halogen bonding with organic bases. Protonated HCFs can form strong mutual hydrogen bonds which give rise to chains, 2D, or 3D networks of the protonated HCF species, and the exact mode of their assembly can be tuned by the strength, steric properties, or the amount of the base. Since the HCFs share many of their electronic properties with other PCMs, as well as with more complex compounds such as nitroprussides, the behavior discovered in this research is likely to also be observed in the whole class of coordination compounds. Thus, on the basis of direct hydrogen bonding, and possibly by combining it with other modes of connecting PCM anions, a new family of Prussian blue analogues could be established.

EXPERIMENTAL SECTION

Synthetic Procedures. Unless stated otherwise, all starting materials (solvents, organic bases, reactants for syntheses) were purchased from commercial sources and used as found.

Hexacyanoferric(II) acid was prepared following a procedure described in the literature.⁸³ Aqueous solution of potassium hexacyanoferrate(II) trihydrate (4.2 g in 35 mL) was acidified with concentrated hydrochloric acid (10 mL). After cooling to about 0 °C, ether (7.0 mL) was added to the mixture to precipitate the acid. The precipitate was redissolved in methanol (5.0 mL) and reprecipitated with another portion of ether (7.0 mL). Yield: 1.40 g (65.2%).

12 was synthesized from 3-aminopyridine and glycerol by a modified procedure from the literature.⁹⁴ A mixture of 3-aminopyridine (3.0 g), glycerol (2.4 mL), concentrated sulfuric acid (1.6 mL), and arsenic(V) oxide (0.5 g) was heated at 170 °C for 5 h. After being cooled to room temperature, the reaction mixture was dissolved in water and neutralized with sodium carbonate (3.24 g). The neutralized mixture was extracted with ether, the extract was dried by sodium sulfate, and the product was obtained by evaporation of ether. Yield: 0.80 g (19%).

All hexacyanoferrates studied in this research were prepared by reactions of hexacyanoferric(II) acid and organic bases, with various molar ratios of bases and the acid (Table 1). This was in general performed by mixing an aqueous solution of hexacyanoferric(II) acid (20 mg in 2 mL of water) with one, two, or more equivalents of the base dissolved in 2 mL of water, methanol, or ethanol, except for **2** and **4**, which were, being liquid, added directly to the aqueous acid. The crystals suitable for X-ray diffraction analysis were obtained after standing for several hours, or by slow evaporation of the solvents over several days.

X-ray Diffraction Measurements and Crystal Structure Refinement. Single crystal diffraction experiments were performed at room temperature on an Oxford Diffraction Xcalibur diffractometer with Sapphire3 CCD detector, using MoK α radiation, except for **XIV**, which was measured on Oxford Diffraction Xcalibur Nova R (microfocus Cu tube) equipped with an Oxford Instruments CryoJet liquid-nitrogen cooling device. The crystal structures were solved using SIR-92⁹⁵ (except for **IV** and **XIV**, where SHELXS⁹⁶ was used) and refined using SHELXL-97. Selected crystallographic data are given in Table S1 in the Supporting Information.

In **IV**, **V**, **VI**, **VII**, **XI**, and **XIV** structural disorder was observed. Carbamate zwitterion in **IV** was modeled assuming conformational disorder, as evident from the differential Fourier electron density maps after locating the main component. Disordered water molecules in **V** and **VII** were modeled as being biperiodically disordered (except for one water molecule in **VII**, which was disordered near the inversion center), as well as one part of the phenantrolium cations in **XIV**. Part of quinolinium cations in **VI**, quinoxaline molecules in **XI**, and the other part of phenantrolium cations in **XIV** were disordered around the inversion centers, and modeled as being in biperiodical disorder with inversion.

All alkyl and aryl hydrogen atoms were placed at calculated positions on parent atoms using the riding model. Whenever possible, hydrogen atoms bonded to oxygen and nitrogen atoms were located from differential Fourier electron density maps and refined isotropically. In **VI**, **VII**, **XIV**, and **XV**, due to disorder and/or poor quality of the crystals, hydrogen atoms could only be partly located from the differential Fourier electron density maps.

ASSOCIATED CONTENT

Supporting Information

The Supporting Information is available free of charge on the ACS Publications website at DOI: 10.1021/acs.cgd.7b01363.

The following files are available free of charge: crystallographic data, detailed descriptions of crystal structures, correlations, and hydrogen bond parameters (PDF)

Accession Codes

CCDC 1541085–1541099 contain the supplementary crystallographic data for this paper. These data can be obtained free of charge via www.ccdc.cam.ac.uk/data_request/cif, or by emailing data_request@ccdc.cam.ac.uk, or by contacting The Cambridge Crystallographic Data Centre, 12 Union Road, Cambridge CB2 1EZ, UK; fax: +44 1223 336033.

AUTHOR INFORMATION

Corresponding Author

*Tel: +385 1 4606371. Fax: +385 1 4606341. E-mail: vstilinovic@chem.pmf.hr

ORCID

Vladimir Stilinović: 0000-0002-4383-5898

Present Address

[†]Synthetic Organic Chemistry – Stratingh Institute for Chemistry, Faculty of Mathematics and Natural Sciences, University of Groningen, Nijenborgh 4, 9747 AG Groningen, The Netherlands.

Funding

We are thankful to the Ministry of Science, Education and Sport of the Republic of Croatia, for funding this research (Grant No. 199-1193079-3069).

Notes

The authors declare no competing financial interest.

ACKNOWLEDGMENTS

We are thankful to Dr. Krešimir Molčanov for X-ray diffraction measurements of **XIV**.

ABBREVIATIONS

HCF, hexacyanoferrate; PCM, polycyanometallate; MOF, metal–organic framework

REFERENCES

- (1) Macquer, P. J. *Dictionnaire de Chimie*, 2nd ed.; Theophile Barrois: Paris, 1778; Vol 1, pp 176–182.
- (2) Macquer, P. J. *Chymisches Wörterbuch, Erster Theil (A–D)*; Weidmannsche Buchhandlung: Leipzig, 1806; pp 311–329.
- (3) Ware, M. J. *Chem. Educ.* **2008**, *85*, 612–621.
- (4) Wilde, R. E.; Ghosh, S. N.; Marshall, B. J. *Inorg. Chem.* **1970**, *9*, 2512–2516.
- (5) Buser, H. J.; Schwarzenbach, D.; Petter, W.; Ludi, A. *Inorg. Chem.* **1977**, *16*, 2704–2710.
- (6) Dunbar, K. R.; Heinz, R. A. Chemistry of Transition Metal Cyanide Compounds: Modern Perspectives. In *Progress in Inorganic Chemistry*; Karlin, K. D., Eds.; John Wiley & Sons, Inc.: Hoboken, NJ, 1996; Vol. 45.
- (7) Karyakin, A. *Electroanalysis* **2001**, *13*, 813–819.
- (8) de Tacconi, N. R.; Rajeshwar, K.; Lezna, R. O. *Chem. Mater.* **2003**, *15*, 3046–3062.
- (9) Kong, B.; Selomulya, C.; Zheng, G.; Zhao, D. *Chem. Soc. Rev.* **2015**, *44*, 7997–8018.
- (10) Wessells, C. D.; Huggins, R. A.; Cui, Y. *Nat. Commun.* **2011**, *2*, 550.
- (11) Lu, Y.; Wang, L.; Cheng, J.; Goodenough, J. B. *Chem. Commun.* **2012**, *48*, 6544–6546.
- (12) Nie, P.; Shen, L.; Luo, H.; Ding, B.; Xu, G.; Wang, J.; Zhang, X. *J. Mater. Chem. A* **2014**, *2*, 5852–5857.
- (13) Pasta, M.; Wessells, C. D.; Liu, N.; Nelson, J.; McDowell, M. T.; Huggins, R. A.; Toney, M. F.; Cui, Y. *Nat. Commun.* **2014**, *5*, 3007.
- (14) Lee, H.-W.; Wang, R. Y.; Pasta, M.; Lee, S. W.; Liu, N.; Cui, Y. *Nat. Commun.* **2014**, *5*, 5280.
- (15) You, Y.; Wu, X.-L.; Yin, Y.-X.; Guo, Y.-G. *Energy Environ. Sci.* **2014**, *7*, 1643–1647.
- (16) Canepa, P.; Gautam, G. S.; Hannah, D. C.; Malik, R.; Liu, M.; Gallagher, K. G.; Persson, K. A.; Ceder, G. *Chem. Rev.* **2017**, *117*, 4287–4341.
- (17) Ferlay, S.; Mallah, T.; Ouahés, R.; Veillet, P.; Verdager, M. *Nature* **1995**, *378*, 701–703.
- (18) Ohba, M.; Ōkawa, H.; Fukita, N.; Hashimoto, Y. *J. Am. Chem. Soc.* **1997**, *119*, 1011–1019.
- (19) Ohba, M.; Usuki, N.; Fukita, N.; Ōkawa, H. *Angew. Chem., Int. Ed.* **1999**, *38*, 1795–1798.
- (20) Verdager, M.; Bleuzen, A.; Marvaud, V.; Vaissermann, J.; Seuleiman, M.; Desplanches, C.; Scuille, A.; Train, C.; Garde, R.; Gelly, G.; Lomenech, C.; Rosenman, I.; Veillet, P.; Cartier, C.; Villain, F. *Coord. Chem. Rev.* **1999**, *190–192*, 1023–1047.
- (21) Ohba, M.; Ōkawa, H. *Coord. Chem. Rev.* **2000**, *198*, 313–328.
- (22) Liu, C.-M.; Gao, S.; Kou, H.-Z.; Zhang, D.-Q.; Sun, H.-L.; Zhu, D.-B. *Cryst. Growth Des.* **2006**, *6*, 94–98.
- (23) Wang, X.-Y.; Avendaño, C.; Dunbar, K. R. *Chem. Soc. Rev.* **2011**, *40*, 3213–3238.
- (24) Coronado, E.; Espallargas, G. M. *Chem. Soc. Rev.* **2013**, *42*, 1525–1539.
- (25) Sato, O.; Iyoda, T.; Fujishima, A.; Hashimoto, K. *Science* **1996**, *272*, 704–705.
- (26) Ohkoshi, S.; Einaga, Y.; Fujishima, A.; Hashimoto, K. *J. Electroanal. Chem.* **1999**, *473*, 245–249.
- (27) Zhang, Y.; Li, D.; Clérac, R.; Kalisz, M.; Mathonière, C.; Holmes, S. M. *Angew. Chem., Int. Ed.* **2010**, *49*, 3752–3756.
- (28) Zhang, Y.-Z.; Ferko, P.; Siretanu, D.; Ababei, R.; Rath, N. P.; Shaw, M. J.; Clérac, R.; Mathonière, C.; Holmes, S. M. *J. Am. Chem. Soc.* **2014**, *136*, 16854–16864.
- (29) Cai, L.-Z.; Chen, Q.-S.; Zhang, C.-J.; Li, P.-X.; Wang, M.-S.; Guo, G.-C. *J. Am. Chem. Soc.* **2015**, *137*, 10882–10885.
- (30) Kuyper, J.; Boxhoorn, G. *J. Catal.* **1987**, *105*, 163–174.
- (31) Balmaseda, J.; Reguera, E.; Rodríguez-Hernández, J.; Reguera, L.; Autie, M. *Microporous Mesoporous Mater.* **2006**, *96*, 222–236.
- (32) MasPOCH, D.; Ruiz-Molina, D.; Veciana, J. *Chem. Soc. Rev.* **2007**, *36*, 770–818.
- (33) Nigrovic, V. *Phys. Med. Biol.* **1965**, *10*, 81–91.
- (34) Kamerbeek, H. H.; Rauws, A. G.; ten Ham, M.; van Heijst, A. N. P. *Acta Med. Scand.* **1971**, *189*, 321–324.
- (35) Parajuli, D.; Takahashi, A.; Noguchi, H.; Kitajima, A.; Tanaka, H.; Takasaki, M.; Yoshino, K.; Kawamoto, T. *Chem. Eng. J.* **2016**, *283*, 1322–1328.
- (36) Kaye, S. S.; Long, J. R. *J. Am. Chem. Soc.* **2005**, *127*, 6506–6507.
- (37) Murray, L. J.; Dincă, M.; Long, J. R. *Chem. Soc. Rev.* **2009**, *38*, 1294–1314.
- (38) Suh, M. P.; Park, H. J.; Prasad, T. K.; Lim, D.-W. *Chem. Rev.* **2012**, *112*, 782–835.
- (39) Takahashi, A.; Tanaka, H.; Parajuli, D.; Nakamura, T.; Minami, K.; Sugiyama, Y.; Hakuta, Y.; Ohkoshi, S.; Kawamoto, T. *J. Am. Chem. Soc.* **2016**, *138*, 6376–6379.
- (40) Ohba, M.; Usuki, N.; Fukita, N.; Ōkawa, H. *Inorg. Chem.* **1998**, *37*, 3349–3354.
- (41) Yuan, A.; Zou, J.; Li, B.; Zha, Z.; Duan, C.; Liu, Y.; Xu, Z.; Keizer, S. *Chem. Commun.* **2000**, *14*, 1297–1298.
- (42) Larionova, J.; Clérac, R.; Donnadiou, B.; Willemin, S.; Guérin, C. *Cryst. Growth Des.* **2003**, *3*, 267–272.
- (43) Shorrock, C. J.; Jong, H.; Batchelor, R. J.; Leznoff, D. B. *Inorg. Chem.* **2003**, *42*, 3917–3924.
- (44) Koner, R.; Nayak, M.; Ferguson, G.; Low, J. N.; Glidewell, C.; Misra, P.; Mohanta, S. *CrystEngComm* **2005**, *7*, 129–132.
- (45) Sieklucka, B.; Podgajny, R.; Przychodzen, P.; Korzeniak, T. *Coord. Chem. Rev.* **2005**, *249*, 2203–2221.
- (46) Przychodzen, P.; Korzeniak, T.; Podgajny, R.; Sieklucka, B. *Coord. Chem. Rev.* **2006**, *250*, 2234–2260.
- (47) Chen, W.-T.; Wang, M.-S.; Cai, L.-Z.; Xu, G.; Akitsu, T.; Akita-Tanaka, M.; Guo, G.-C.; Huang, J.-S. *Cryst. Growth Des.* **2006**, *6*, 1738–1741.
- (48) Wang, Z.-X.; Zhang, P.; Shen, X.-F.; Song, Y.; You, X.-Z.; Hashimoto, K. *Cryst. Growth Des.* **2006**, *6*, 2457–2462.
- (49) Katz, M. J.; Kaluarachchi, H.; Batchelor, R. J.; Schatte, G.; Leznoff, D. B. *Cryst. Growth Des.* **2007**, *7*, 1946–1948.
- (50) Li, J.-R.; Chen, W.-T.; Tong, M.-L.; Guo, G.-C.; Tao, Y.; Yu, Q.; Song, W.-C.; Bu, X.-H. *Cryst. Growth Des.* **2008**, *8*, 2780–2792.
- (51) Yuan, A.-H.; Lu, R.-Q.; Zhou, H.; Chen, Y.-Y.; Li, Y.-Z. *CrystEngComm* **2010**, *12*, 1382–1384.
- (52) Mittal, R.; Zbiri, M.; Schober, H.; Achary, S. N.; Tyagi, A. K.; Chaplot, S. L. *J. Phys.: Condens. Matter* **2012**, *24*, 505404.
- (53) Nowicka, B.; Korzeniak, T.; Stefańczyk, O.; Pinkowicz, D.; Choraży, S.; Podgajny, R.; Sieklucka, B. *Coord. Chem. Rev.* **2012**, *256*, 1946–1971.
- (54) Ferlay, S.; Dechambenoit, P.; Kyritsakas, N.; Hosseini, M. W. *Dalton Trans.* **2013**, *42*, 11661–11671.
- (55) Alexandrov, E. V.; Virovets, A. V.; Blatov, V. A.; Peresyphina, E. V. *Chem. Rev.* **2015**, *115*, 12286–12319.
- (56) Hill, J. A.; Thompson, A. L.; Goodwin, A. L. *J. Am. Chem. Soc.* **2016**, *138*, 5886–5896.
- (57) Ferlay, S.; Bulach, V.; Félix, O.; Hosseini, M. W.; Planeix, J. M.; Kyritsakas, N. *CrystEngComm* **2002**, *4*, 447–453.
- (58) Hosseini, M. W. *Coord. Chem. Rev.* **2003**, *240*, 157–166.
- (59) Hosseini, M. W. *Acc. Chem. Res.* **2005**, *38*, 313–323.
- (60) Dechambenoit, P.; Ferlay, S.; Hosseini, M. W. *Cryst. Growth Des.* **2005**, *5*, 2310–2312.
- (61) Dechambenoit, P.; Ferlay, S.; Hosseini, M. W.; Planeix, J.-M.; Kyritsakas, N. *New J. Chem.* **2006**, *30*, 1403–1410.
- (62) Dechambenoit, P.; Ferlay, S.; Hosseini, M. W.; Kyritsakas, N. *Chem. Commun.* **2007**, *44*, 4626–4628.
- (63) Dechambenoit, P.; Ferlay, S.; Kyritsakas, N.; Hosseini, M. W. *J. Am. Chem. Soc.* **2008**, *130*, 17106–17113.
- (64) Dechambenoit, P.; Ferlay, S.; Donnio, B.; Guillon, D.; Hosseini, M. W. *Chem. Commun.* **2011**, *47*, 734–736.
- (65) Dechambenoit, P.; Ferlay, S.; Kyritsakas, N.; Hosseini, M. W. *CrystEngComm* **2011**, *13*, 1922–1930.
- (66) Hazra, A.; Gurunatha, K. L.; Maji, T. K. *Cryst. Growth Des.* **2013**, *13*, 4824–4836.
- (67) Derossi, S.; Brammer, L.; Hunter, C. A.; Ward, M. D. *Inorg. Chem.* **2009**, *48*, 1666–1677.

- (68) Ormond-Prout, J. E.; Smart, P.; Brammer, L. *Cryst. Growth Des.* **2012**, *12*, 205–216.
- (69) Troff, R. W.; Mäkelä, T.; Topić, F.; Valkonen, A.; Raatikainen, K.; Rissanen, K. *Eur. J. Org. Chem.* **2013**, *2013*, 1617–1637.
- (70) Christopherson, J.-C.; Potts, K. P.; Bushuyev, O. S.; Topić, F.; Huskić, I.; Rissanen, K.; Barrett, C. J.; Friščić, T. *Faraday Discuss.* **2017**, *203*, 441.
- (71) Bär, E.; Fuchs, J.; Rieger, D.; Aguilar-Parrilla, F.; Limbach, H.-H.; Fehlhammer, W. P. *Angew. Chem., Int. Ed. Engl.* **1991**, *30*, 88–90.
- (72) Fehlhammer, W. P.; Fritz, M. *Chem. Rev.* **1993**, *93*, 1243–1280.
- (73) Nadele, D.; Schweda, E. *Z. Kristallogr. - Cryst. Mater.* **1999**, *214*, 358–361.
- (74) Gorelsky, S. I.; Ilyukhin, A. B.; Kholin, P. V.; Kotov, V. Y.; Lokshin, B. V.; Sapoletova, N. V. *Inorg. Chim. Acta* **2007**, *360*, 2573–2582.
- (75) Pierrot, M.; Kern, R.; Weiss, R. *Acta Crystallogr.* **1966**, *20*, 425–428.
- (76) Haser, R.; Pierrot, M.; de Broin, C.-É. *C. R. Acad. Sci.* **1969**, *268*, 51.
- (77) Haser, R.; de Broin, C. E.; Pierrot, M. *Acta Crystallogr., Sect. B: Struct. Crystallogr. Cryst. Chem.* **1972**, *28*, 2530–2537.
- (78) Haser, R.; Pierrot, M. *Acta Crystallogr., Sect. B: Struct. Crystallogr. Cryst. Chem.* **1972**, *28*, 2538–2542.
- (79) Haser, R.; Pierrot, M. *Acta Crystallogr., Sect. B: Struct. Crystallogr. Cryst. Chem.* **1972**, *28*, 2542–2547.
- (80) Haser, R.; Penel, C.; Pierrot, M. *Acta Crystallogr., Sect. B: Struct. Crystallogr. Cryst. Chem.* **1972**, *28*, 2548–2554.
- (81) Pauling, L.; Pauling, P. *Proc. Natl. Acad. Sci. U. S. A.* **1968**, *60*, 362–367.
- (82) Keen, D. A.; Dove, M. T.; Evans, J. S. O.; Goodwin, A. L.; Peters, L.; Tucker, M. G. *J. Phys.: Condens. Matter* **2010**, *22*, 404202.
- (83) Brauer, G. *Handbook of Preparative Inorganic Chemistry*, 2nd ed.; Academic Press: New York, 1963; Vol. 1, p 1509.
- (84) Beck, M. T. *Pure Appl. Chem.* **1987**, *59*, 1703–1720.
- (85) Musgrave, T. R.; Mattson, C. E. *Inorg. Chem.* **1968**, *7*, 1433–1436.
- (86) Hall, H. K., Jr. *J. Phys. Chem.* **1956**, *60*, 63–70.
- (87) Cooney, A. P.; Crampton, M. R.; Golding, P. J. *Chem. Soc., Perkin Trans. 2* **1986**, *6*, 835–839.
- (88) Khalil, M. M.; Mahmoud, R. K. *J. Chem. Eng. Data* **2008**, *53*, 2318–2327.
- (89) Albert, A.; Goldacre, R.; Phillips, J. *J. Chem. Soc.* **1948**, 2240–2249.
- (90) Mesmin, C.; Liljenzin, J.-O. *Solvent Extr. Ion Exch.* **2003**, *21*, 783–795.
- (91) Bruckenstein, S.; Kolthoff, I. M. *J. Am. Chem. Soc.* **1956**, *78*, 2974–2979.
- (92) Albert, A.; Phillips, J. N. *J. Chem. Soc.* **1956**, 1294–1304.
- (93) Irving, H.; Mellor, D. H. *J. Chem. Soc.* **1962**, *0*, 5222–5237.
- (94) Bobrański, B.; Sucharda, G. *Ber. Dtsch. Chem. Ges. B* **1927**, *60*, 1081–1084.
- (95) Altomare, A.; Cascarano, G.; Giacovazzo, C.; Guagliardi, A. *J. Appl. Crystallogr.* **1993**, *26*, 343–350.
- (96) Sheldrick, G. M. *Acta Crystallogr., Sect. A: Found. Crystallogr.* **2008**, *64*, 112–122.